American Journal of
Biomedical Science & Research

www.biomedgrid.com
ISSN: 2642-1747

Research Article

Use of Simple Binary Co-xCr Alloys (0≤x≤30wt.%) for Exploring the Influence of the Chromium Content in Dental Cobalt-Based Alloys on Their Passivation Behavior in a Fusayama Artificial Saliva

Patrice Berthod*, Estelle Kretz and Thierry Schweitzer

Institute Jean Lamour (UMR CNRS 7198), Campus Artem, France

***Corresponding author:** Patrice Berthod, Institute Jean Lamour (UMR CNRS 7198), 2 allée André Guinier, Campus Artem, B.P. 50840, F-54011 NANCY Cedex, France.

To Cite This Article: *Patrice Berthod, Use of Simple Binary Co-xCr Alloys (0≤x≤30wt.%) for Exploring the Influence of the Chromium Content in Dental Cobalt-Based Alloys on Their Passivation Behavior in a Fusayama Artificial Saliva. Am J Biomed Sci & Res. 2020 - 7(1). AJBSR.MS.ID.001109. DOI:* 10.34297/AJBSR.2020.07.001109.

Received: January 09, 2020; **Published:** January 24, 2020

Abstract

More and more Predominantly Base alloys are used instead the expensive dental alloys containing high concentration in noble metals. Among these PB alloys the ones based on cobalt and chromium are rather interesting since they bring high mechanical resistance, and do not risk induce any nickel release in mouth. Their corrosion resistance is due to the presence of chromium the content of which may be optimized. In this work contribution to a better knowledge of the critical Cr content to necessarily exceed for a corrosion resistance high enough is done by exploring the direct relationship between the corrosion behavior and the Cr content, by choosing a particularly aggressive artificial saliva and a series of binary alloys with an increasing Cr content, in order to exclude all other possible parameters susceptible to interfere. The different electrochemical results - free potential follow-up, Stern-Geary results and the cyclic polarization curves - demonstrate that 20wt.%Cr should be enough to allow cobalt-based dental alloys rapidly developing a protective passivation layer and showing a good resistance against corrosion in the buccal milieu. This suggests that the current chromium contents of commercial cobalt-based dental alloys may be lowered down to this threshold value without loss of their good corrosion resistance.

Keywords: Prosthetic Dentistry; Cobalt Alloys; Chromium Content; Corrosion Behavior; Fusayama Saliva; Electrochemical Techniques

Introduction

Some dental prostheses involve the use of metallic alloys. This is for example the case of fixed partial dentures in which metallic alloys of different natures present under the cosmetic ceramic part and covered to be out from view, brought the major part of the mechanical resistance to the compressive and flexural solicitations induced by mastication. Alloys based on cobalt and chromium belong to a the Predominantly Base (PB) dental alloys category, which co-exists beside (Au, Pt, Pd…)-rich alloys of the Noble (N) and High Noble (HN) families, as alternative cheaper materials for dental restoration. As the other PB alloys which are based on nickel and chromium, these cobalt alloys may bring high mechanical properties and good corrosion behavior but with less risk of allergy (in case of nickel release in mouth). The chemical compositions of the cobalt-chromium PB alloys are generally complex since they may contain also tungsten, gallium, rhenium, aluminum… in addit ion to chromium the content of which may furthermore vary over a rather broad range (e.g. from 20 to 35wt.%Cr [1] in commercial alloys. Prosthetic pieces in Co-based PB alloys are generally prepared by casting (e.g. alloy melted by torch and driven in molds by centrifugal casting), but they may be also synthesized following various other elaboration routes (milling, selective laser melting… [2]). Cobalt-based alloys are known for their good mechanical behavior under many kinds of stresses [3], static [4] or dynamic [5,6].

Unfortunately, the alloys of the cobalt-chromium family are possibly not safe from corrosion [7], may be because systematic

studies concerning the influence of the chromium content are seemingly lacking. Binary and ternary alloys with Co and Cr as major elements were considered to investigate microstructures and mechanical/chemical properties [8], but not the corrosion properties in complex electrolytes imitating human saliva. Knowing how the corrosion behavior may vary with the chromium content can be considered as fundamental, even if many other parameters characterizing an alloy (other major elements present, minor elements, grain size, hardening state…) may also influence and more or less hide the sole effect of Cr.

This work aims to isolate the influence of the chromium content from the ones of all the chemical composition or the fabrication process factors, in order to favor the direct observation of how the corrosion behavior depends on the chromium content as single varying parameter. This was done by elaborating in a controlled manner a series of binary alloys, by preparing both electrode and electrolyte following a procedure strictly applied, and by carrying out the electrochemical tests repeatably by fixing all conditions. So the single input data was the chromium content (with six alloys with a Cr content of 0 to 30wt.% by slices of 5wt.%) and the output results were the initial behavior shortly after immersion and the response to severe anodic polarization followed by its progressive suppression.

Materials and Methods

Preparation of the Alloys and Melting Procedure

The work started by the elaboration of a series of seven cobalt or cobalt-chromium alloys: pure Co ("0Cr"), Co-5%Cr ("5Cr"), Co-10%Cr ("10Cr"), Co-15%Cr ("15Cr"), Co-20%Cr ("20Cr"), Co-25%Cr ("25Cr") and Co-30%Cr ("30Cr"), all Cr contents being in weight percent (wt.%) and cobalt being the balance part. The starting chemical elements were pure cobalt and pure chromium, both bought by Alfa Aesar with a 99.9% purity. The adequate masses were weighed using a precision electronic balance (accuracy: ± 0.1mg) in order to obtain a total weight of 40 grams for each alloy.

The synthesis of each alloy started by putting the metallic charges in the metallic crucible of an induction furnace (CELES, France). This crucible, made of copper, was segmented to hinder the induced current circulation, and internally cooled by a continuous circulation of water maintained at ambient temperature. This permanent cooling aimed to avoid heating due to the Foucault currents induced by the electromagnetic field and by the proximity of the molten alloy. The Co and Cr charges being placed in the copper crucible, a silica tube was positioned around the crucible, between it and the copper coil (itself cooled by an internal continuous water flow) in which the alternative current will circulate during melting. The fusion chamber being closed, pumping was carried out until obtaining an internal pressure of about 5×10^{-2} millibars. Pure argon was then injected to rise the internal pressure up to 0,8 atm. Pumping followed by Ar injection were applied two times more and the preparation of the final atmosphere was terminated by supplementary addition of pure Ar up to 300 millibars. The gaseous environment of pure argon with a purity close to the one of the origin Ar bottle with a pressure high enough allowed avoiding both oxidation of Co and notably Cr during the heating, melting, isothermal stage and cooling, and the evaporation of Co and Cr in the chamber.

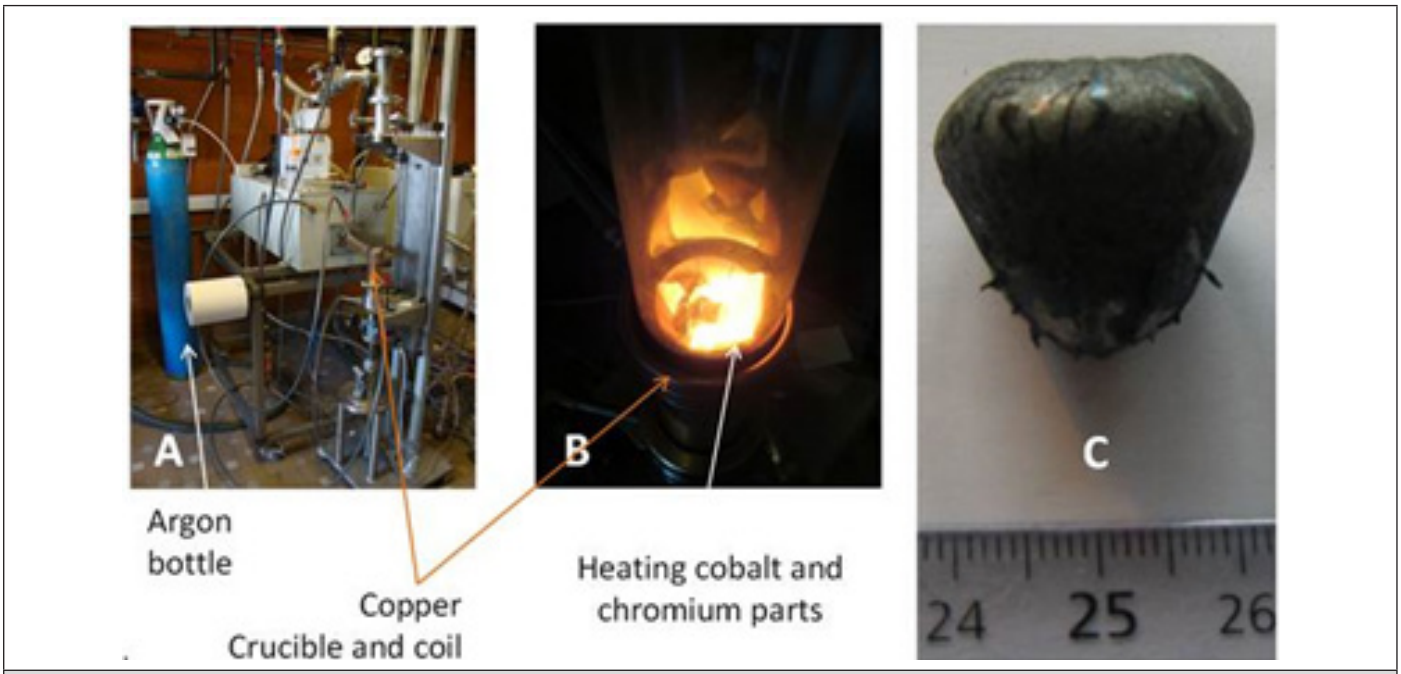

Figure 1: Elaboration of the alloys: the used furnace and its environment (A), the cobalt and chromium parts during their heating and start of melting (B) and example of an obtained ingot (C).

The injected voltage progressively increased from 0 to 4 000 Volts (total duration: about 2 minutes) for a frequency of the resulting current (several Amperes) of about 110 000 Hertz. This provoked the heating of both Co and Cr, the melting of Co and the dissolution of Cr in the molten Co. An isovoltage stage at 4 kV-10 kHz was maintained for 5-minute s to favor the chemical homogenization of the alloy. A progressive decrease in injected voltage allowed the cooling of the levitating liquid alloy, its solidification and its solid-state cooling. After less an hour, the obtained ingot was cold enough to be removed from the furnace and handled. Three photographs illustrate the elaboration process in Figure 1.

Preparation of samples for all characterizations

Each obtained ingot was sawed using a metallographic saw equipped with abrasive wheel. A part was kept for the metallographic characterization and another part for preparing an electrode for the corrosion experiments. Before embedding the first part was just kept in its present state while the second part was preliminarily joined to the emerging metallic part of a plastic-covered copper electrical wire, at a location opposite to the plane surface. Both were embedded in a cold resin mixture (ESCIL, France) in a plastic mold. After about 4 hours the resin was rigidified enough to allow extraction out of the mold and both samples were ground with SiC papers from #120 to #2400-grit, cleaned by ultrasonic vibrations and polished with textile enriched with 1µm abrasive particles until mirror-like state for the emerging metallic surfaces.

Metallographic and Hardness Characterization

Each of the seven metallographic samples was observed with a JSM-6010LA (JEOL, Japan) scanning electron microscope (SEM) in Back Scattered Electrons mode (BSE) to specify the as-cast microstructures of the alloys, and to control their chemical heterogeneity or homogeneity with the help of the Energy Dispersion Spectrometry (EDS) device attached to the SEM. The same metallographic samples were also used to measure the hardness of the as-cast alloys. Five indentations were performed per alloy according to the Vickers method (load: 10kg), in randomly chosen locations. The apparatus which was used was a Testwell Wolpert machine.

Electrochemical experiments

The experimental apparatus exploited for specifying the corrosion behavior of the alloys was composed of:

a. A potensiostat (model 263A, EG&G Instruments / Princeton Applied Research)

b. A computer containing the PowerSuite software driving the potensiostat and allowing exploiting the measurements/ results

c. A double-walled cell through which permanently circulated 38°C-water

d. A Julabo F32 apparatus the role of which was to maintain the water flow crossing the cell double-wall at 38 °C

e. Three electrodes: the working electrode the preparation of which is described above, a platinum auxilliary electrode and a potential-reference Saturated Calomel electrode.

The working electrode was placed in the bottom part of the cell, with its planar metallic part oriented upward and parallel to the platinum disk of the auxiliary electrode (distance between them: about 5mm). The electrolyte of study which was chosen was the Fusayama artificial saliva, the composition of which is presented in Table 1. This solution is commonly used for the corrosion characterization of all types of dental alloys, from the High Noble and Noble categories [9-11] to different kinds of Predominantly Base alloys [12-14]. Its pH being a major factor involved in the aggressiveness of an artificialsaliva (more corrosive in case of acidic pH), special care is to be given to it. Dental plaque pH may vary depending on the dental oral care and food habit [15,16]. In the present case, after its preparation, our Fusayama saliva was acidified to decrease its pH down to 2.3, pH recommended for such corrosion studies [17].

Table 1: Chemical composition of the Fusayama artificial saliva (pH=2.3).

Substance	NaCl	KCl	$CaCl_2$, $2H_2O$	NaH_2PO_4, $2H_2O$	Na_2S, $9H_2O$	Urea
Content in saliva (mg/L)	400	400	906	690	5	1000
Purity	≥ 99.5%	≥ 99%	≥ 99%	≥ 99%	≥ 98%	≥ 99.5%
Supplier	AnalaR Normapur®	Carl Roth	Sigma-Aldrich	Sigma-Aldrich	Alfa Aesar	Carl Roth

The electrochemical tests were of three types:

i. Free potential (E_{ocp}) follow-up for 2 hours after immersion

ii. Polarization resistance (Rp) measurements by applying the Stern-Geary method; polarization from Eocp-20mV to Eocp+20mV with a 10mV/min rate (performed two times: after 1 hour of immersion, and after 2 hours)

iii. Cyclic polarization consisting of an increase of applied potential at 1mV/s from E_{ocp} -150mV up to Eocp +1,23V, followed by its decrease at -1mV/s down to its initial value.

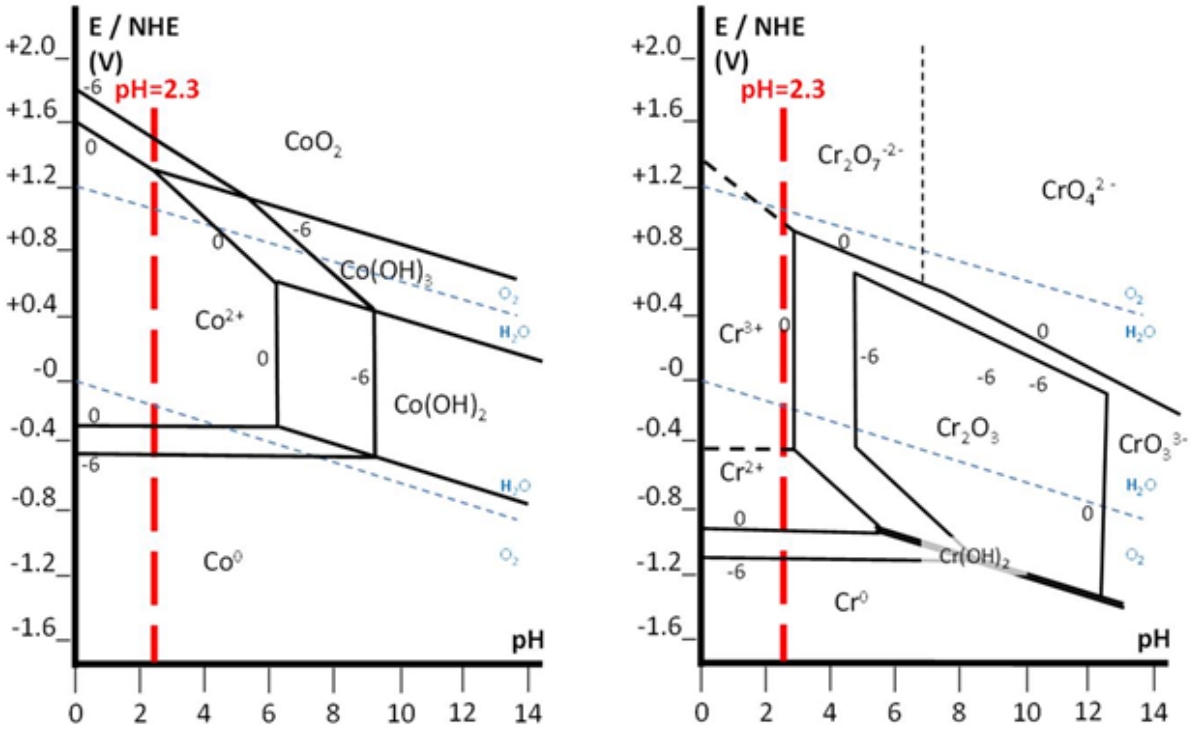

Figure 2: E-pH diagrams of cobalt (left) and of chromium (right).

These results will be compared with the Pourbaix diagrams of cobalt and of chromium. These later ones are reminded in Figure 2.

Results

Elaboration, Metallographic Characterization and Hardness of the Obtained Alloys

Despite the high refractoriness of each of the two alloys constituting the future binary alloys (1490 ± 1°C for Co, 1890±10°C fo r Cr [18]) no problem occurred for the total melting of the alloys, even for the ones the richest in Cr. During heating the cobalt parts started melting, after temperature came above 1500°C. A little later the Cr parts were dissolving in molten cobalt, until their total disappearance. The isothermal stage, maintained for several minutes at about 1600°C, allowed good chemically homogenizatio n of the liquid alloys, as later demonstrated by chemical analysis with the SEM. Solidification took about one minute, followed by solid state cooling. After extraction out of the cold crucible, cutting and metallographic preparation, the mirror-like state samples appeared as single-phased when observed with the SEM in BSE mode (Figure 3). Dispersed spot EDS analyses demonstrated that all the alloys were chemically homogenous, with Cr contents very close to the full frame EDS measurement results given in Table 2.

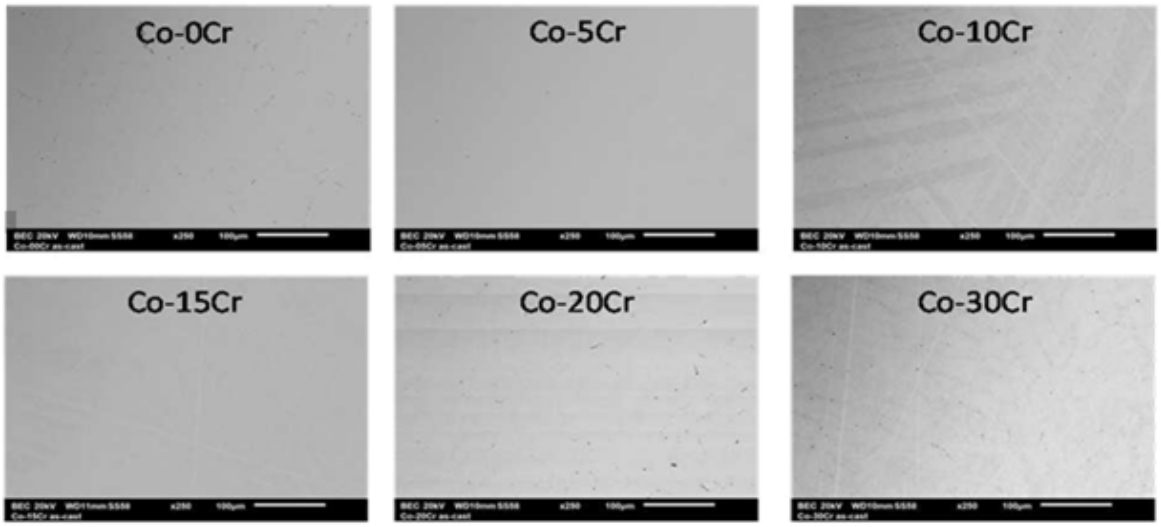

Figure 3: Microstructures of six out of the seven alloys (SEM/BSE mode).

Table 2: Real chemical compositions of the alloys of the study (± 1wt.%).

Alloy	5Cr	10Cr	15Cr	20Cr	25Cr	30Cr
Cr contents (wt.%) as	5	11	16	22	26	31

Five values of Vickers hardness were obtained per alloy for a 10kg-load. The average and standard deviation values are displayed in Table 3. The addition of more and more chromium obviously induces a rather regular increase in hardness, from about 140 to 250 Hv_{10kg}.

Table 3: Hardness of the studied alloys (5 Vickers indentations under a load equal to 10kg).

Alloy	0Cr	5Cr	10Cr	15Cr	20Cr	25Cr	30Cr
Average of 5 values	137	198	189	228	221	251	254
Standard deviation	13	20	9	23	7	5	13

Electrochemical Results / Corrosion Behavior: Qualitative and Semi-Quantitative Results

The first data obtained concerning the behavior in corrosion of the studied alloys are their equilibrium potentials (or open circuit potential: E_{ocp}) with the artificial saliva and their evolutions with time (Figure 4). It appears that the seven alloys can be divided in four groups each characterized by a specific behavior. The initial potentials of the two Cr-poorest alloys (pure Co and the Co-5wt.%Cr alloy) are rather low (close to -100mV versus the Normal Hydrogen Electrode). They decrease a little before increasing for stabilizing at - 70/-60 mV/NHE. The alloys containing 10 and 15 wt. %Cr constitute a second group. Their initial potential is higher (around -25mV / NHE) than the ones of the former alloys but they rapidly decrease before stabilizing around - 100mV/NHE. The two following alloys (Co-20wt.%Cr and Co-25wt.%, third group) remain at a level significantly higher than the previous alloys: after an initial E_{ocp} around +25mV/NHE their potentials stabilize at 0mV/NHE. And finally, the chromium-richest alloy (with 30wt.%Cr) starts at about +20mV/NHE and its E_{ocp} potential steadily increases it reaches about +100mV/NHE after 2 hours of immersion. A common point between all the alloys is that all these open circuit potentials, varying with the Cr content in alloy and with the immersion time, stay in the corrosion domain of Co and in the corrosion domain of Cr, as graphically shown in the same Figure 4 by the colored areas showing the predominance domains of the +II and +III oxidized states of both elements. Thereby all alloys are expected to be in an active state.

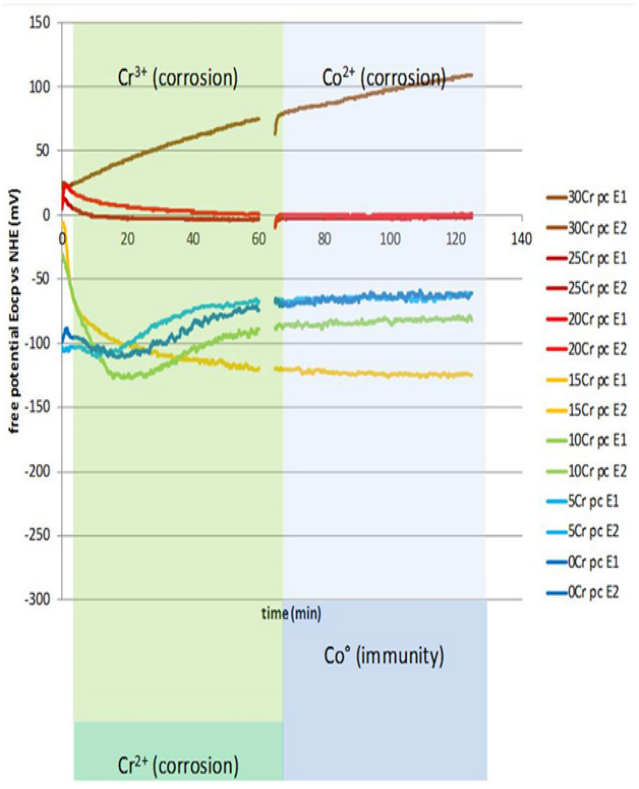

Figure 4: Free potential evolution of the seven alloys plotted versus time during 2 × 1 hour prior to cyclic polarization.
Note: Cr^{2+} (corrosion), Co° (immunity).

After one hour of immersion with E_{ocp}-following a first polarization over a 40mV-range centered on the current value of E_{ocp} was applied in order to specify the polarization resistance according to the Stern-Geary method. This was done a second time, after 2 hours of immersion, just before cyclic polarization. The exploitation of the obtained curves led to the values of Rp given in Table 4. The results are obviously of two levels: 1kΩ × cm^2 for the alloys containing 15 wt.%Cr or less, and several hundreds of 1kΩ × cm^2 for the alloys with 20 wt.%Cr and more. This suggests that the four Cr-poorest alloys were permanently in an active state during the 2 hours-immersion while the three Cr-richest ones became passive during the first hour of immersion .

Table 4: The two values of the polarization resistance issued from Stern-Geary during the two hours of immersion prior to cyclic polarization Tafel experiment (Rp1: after 1h of immersion, Rp2: after 2h of immersion).

Alloys	0Cr	5Cr	10Cr	15Cr	20Cr	25Cr	30Cr
Rp1 (Ω×cm^2) 1151		840	957	894	235797	224669	349036
Rp2 (Ω×cm^2)	1116	747	1009	970	333133	304010	552138

These assumptions found confirmation in the potential-increasing parts of the curves plotted with the potential and current densities acquired during the cyclic polarization carried out just several minutes after the last Stern-Geary experiment. Indeed, the two Cr-poorest alloys (0 and 5 wt.%Cr only) were obviously in an active state as demonstrated with the low potential parts of the curves located in the high current densities part of the graph (Figure 5). Furthermore, no passivation seemed to take place for higher potentials. The alloys containing 10 and 15 wt.%Cr are characterized by the low potential part of the E-increasing curve situated too in the high current density part of the graph (Figure 6). But, unlike the two previous alloys, passivation occurs as soon as the current density exceeds a threshold value (anodic peak, critical current of passivation) and the applied potential reaches the passivation potential. The three Cr-richest alloys do not show such behavior since they are obviously already passivated as suggested by the low-potential parts of the E-increasing curve which are in the low current density part of the graph (Figure 7). These observations let think that the passivation of the alloys happens more (Co-10 and 15 wt.% Cr: during cyclic passivation) or less (20 wt.%Cr and more: during the initial free immersion) late as soon as the chromium content is high enough. The obtained passivation layer is then very stable since no de-passivation occurred during the E-decreasing part of the cyclic polarization runs.

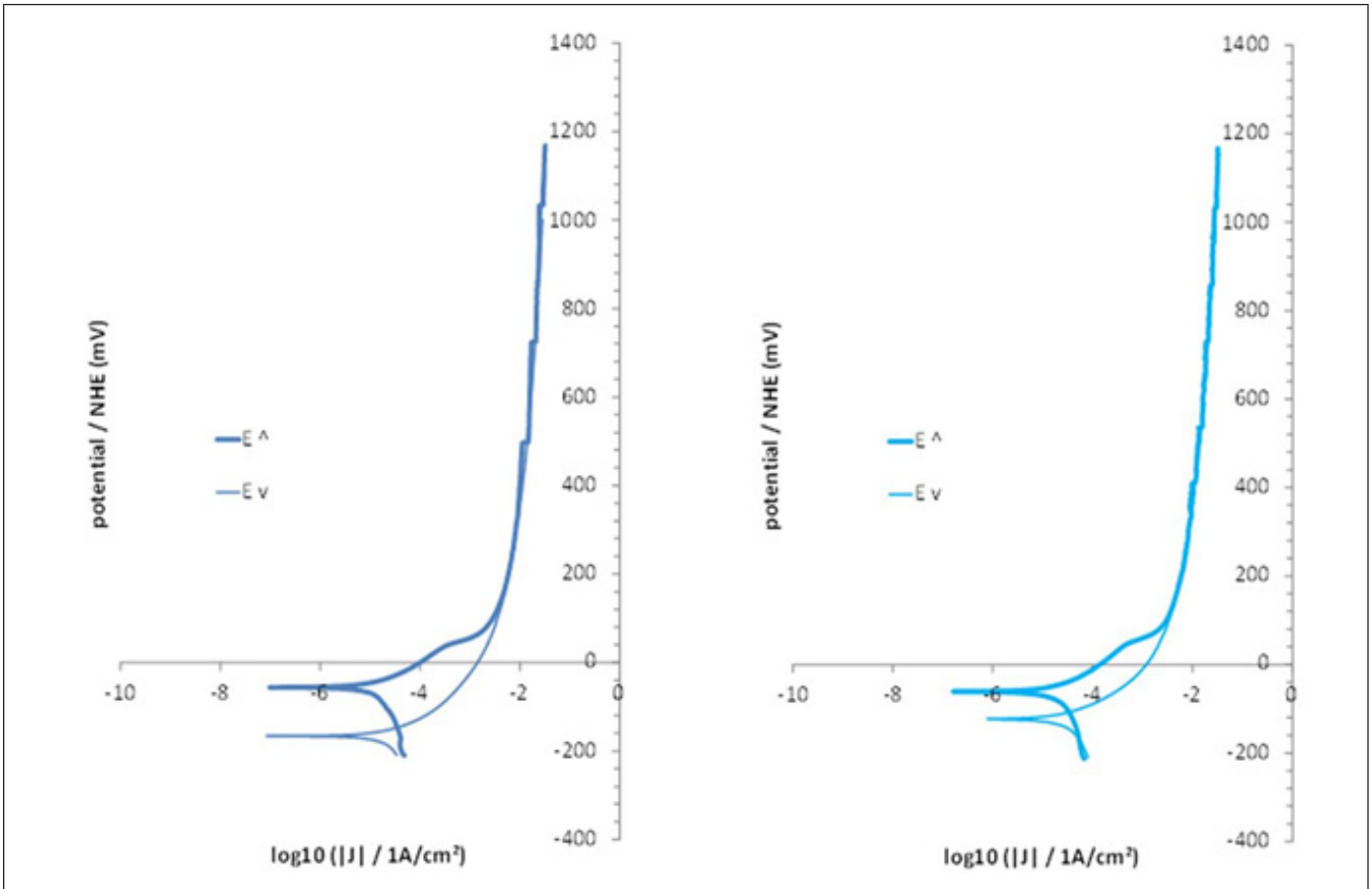

Figure 5: E-J curves obtained during the cyclic polarization of Cr-lowest alloys (left: Co-0Cr, right: Co-5Cr).

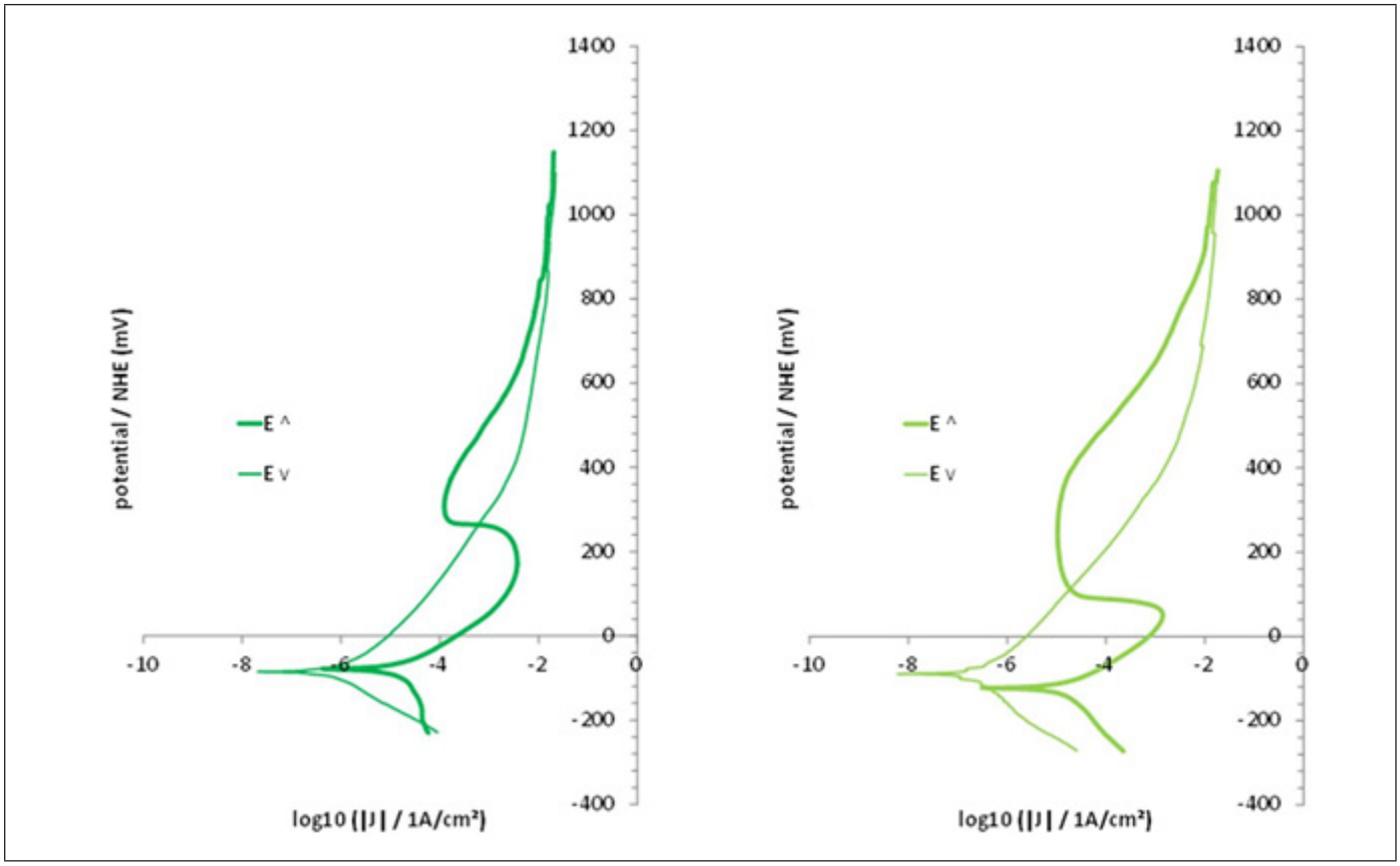

Figure 6: E-J curves obtained during the cyclic polarization of the two alloys with intermediate Cr contents (left: Co-10Cr, right: Co-15Cr).

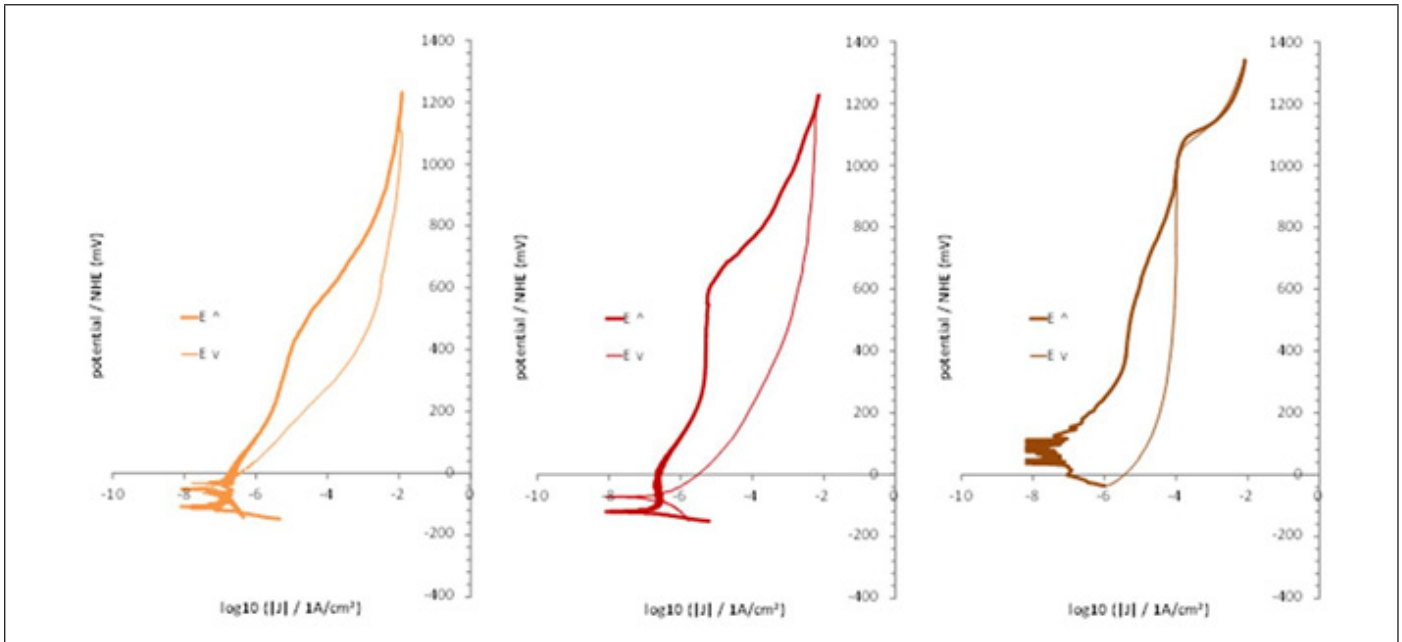

Figure 7: E-J curves obtained during the cyclic polarization of the two of the three Cr-richest alloys (left: Co-20Cr, middle: Co-25Cr, right: Co-30Cr).

Electrochemical Results / Corrosion Behavior: Quantitative Results

The cyclic polarization curves were exploited to specify some data characterizing the easiness of passivation ($J_{critical}$ and E_{passiv}) and the corrosion resistance in passive state (J_{passiv}). $J_{critical}$ is the critical current that is compulsory to exceed by the alloy in order to get passive and E_{passiv} is the corresponding passivation potential to exceed. A better easiness to become passive is demonstrated by a

lower critical current (or a smaller/less extended anodic peak) and by a lower passivation potential easier to obtain in case of low presence of oxidants. J_{passiv} is the anodic current at high potential when the alloy is covered by a passivation layer: this one is more protective if the passivation current is lower. One also made use of the Tafel-type of the E-increasing and E-decreasing parts in the neighborhood of the cathodic→anodic and anodic→cathodic transitions respectively, to apply the Tafel method in order to assess the values of corrosion density of current (J_{corr}) and of corrosion potential (E_{corr}) before and after the polarization at high potential. The determination of all these data is explained in Figure 8 and the obtained values listed in Table 5.

Table 5: Values of the characteristic values of potential and current density noted on the potential-increasing parts of the cyclic polarisation curves.

E increasing part	E_{corr} (mV/NHE)	J_{corr} (µA/cm²)	$J_{critical}$ (mA/cm²)	E_{passiv} (mV/NHE)	J_{passiv} (µA/cm²)
0Cr	-56	11	/	/	/
5Cr	-61	26	/	/	/
10Cr	-81	14	3.7	265	126
15Cr	-121	16	1.3	87	11
20Cr	-47	0.081	/	/	/
25Cr	-120	0.098	/	/	/
30Cr	81	0.026	/	/	/

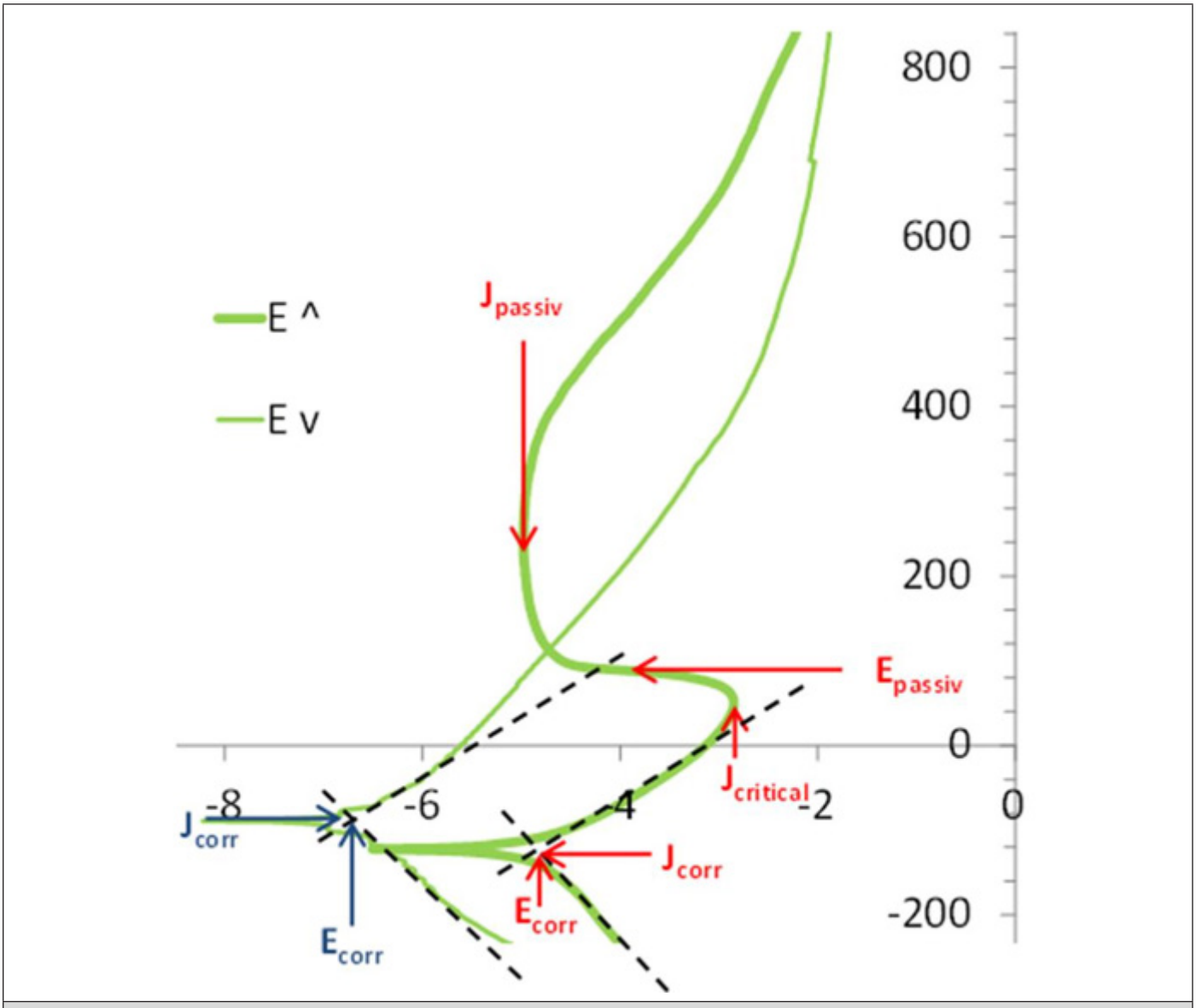

Figure 8: Description of the key data measured on the cyclic polarization curves.

With corrosion currents of more than 10 µA/cm^2 before polarization at high potential one confirms that the alloys containing 15wt.%Cr or less are in an active state. The initial current densities of corrosion of the alloys containing more chromium are much lower: less than 0.1 µA/cm^2, as is to say more than two orders of magnitude below. The 30wt.%Cr-containing alloy presents particularly slow corrosion with less than 30nA/cm^2. This confirms that the alloys with 15wt.%Cr and more became passivated prior to the beginning of the cyclic polarization run, during the 2 hours – E_{ocp} follow-up.

Near the end of the cyclic polarization curves the Tafel features characterizing the last parts of the E-decreasing curves were also exploited (Table 6). For the Cr-lowest alloys (which did not passivate) as well as for the Cr-richest ones (which were already passivated before start of cyclic passivation), this led to corrosion current densities which are more or less higher than the initial J_{corr} values (e.g. 23µA/cm^2 against only 11 initially for the Cr-free alloy and 0.49µ/cm^2 against only around 0.1 for the 25wt.%Cr-containing alloy). This is due to the oxidation of the solvent (water) in gaseous oxygen (additional O2, also dissolved in the solution) which led locally to a higher concentration in strong oxidant species. For the alloys with intermediate Cr contents (10 and 15 wt.%Cr), such comparison cannot be done since the states before and after polarization at high potential are not the same: active state before and passive state after. The current densities of corrosion are, in both cases, much lower after polarization at high potential than before (e.g. 0.3µA/cm^2 against one hundred times more before, for the 15wt.%Cr-containing alloy). One can additionally mention that, with both a critical current of passivation lower than the 10wt.%Cr-containing alloy's one (1.3 against 1.7mA/cm^2) and a lower passivation potential (+87 against +265mV/NHE), the 15wt.%Cr-containing alloy is easier to passivate.

Table 6: Values of the characteristic values of potential and current density noted on the potential-decreasing parts of the cyclic polarisation curves.

E decreasing part	Ecorr (mV/NHE)	Jcorr (µA/cm^2)
0Cr	-166	23
5Cr	-123	28
10Cr	-85	0.56
15Cr	-88	0.31
20Cr	-40	0.11
25Cr	-72	0.49
30Cr	/	/

Discussion

Using high purity cobalt and chromium allowed obtaining a series of binary cobalt-chromium alloys for this study devoted to the specific role of the chromium content. Using high frequency induction melting in cold crucible allowed obtaining equiaxed fine-grained polycrystalline alloys with a good chemical homogeneity (electromagnetic stirring), verified by EDS with the SEM. All alloys, even the Cr-richest ones, were single-phased although a second phase may be expected for the higher Cr contents according to the cobalt-chromium phase diagram. The high temperature structure was kept thanks to the rather rapid solidification and solid-state cooling. The microstructures of each alloy were consequently composed of only two components: the solid solution of chromium in cobalt (or cobalt only for the single Cr-free alloy) and the unavoidable grain boundaries, the cumulative surface fraction of which was necessarily not significant beside grains. So, the studied global electrochemical response of each alloy was only the sum of the individual contributions of all the randomly oriented crystals of cobalt solid solution with Cr homogeneously dispersed in substitution of some Co atoms. By comparison with real alloys, the present alloys were thus much simplier and suitable to an exploration of the role of chromium without any interference with other possible influencing factors. Special care was given to the samples and electrodes preparations and for the preparation of the experimental apparatus for the electrochemical experiments to do not lose this advantage brought by this special nature of the alloys. This is thus not surprising that a rather clear dependence, on the Cr content, of all the studied electrochemical properties was successfully demonstrated.

The first observations which were done concern the free potential of the alloy immersed in the electrolyte. The observed behaviors of the alloys allowed classifying them in two categories, by considering the average level of the free potential after about half an hour. The four Cr-poorest alloys (0 £ Cr ££ 15 wt.%) staid at a level about 100mV under the potential at which the three Cr-richest alloys Cr content from 20 to 30 wt.% finished themselves to (more or less) stabilize. The Stern-Geary runs, carried out after 1 hour and 2 hours after immersion gave more information by demonstrating that the corrosion rates of the three Cr-richest alloys were much lower than the ones of the four Cr-poorest alloys (polarization resistances several hundred times higher). Obviously higher Eocp and higher Rp values witnessed of an active state of the alloys with Cr content equal or lower than 15wt.% and of a passive state for the alloys with 20wt.%Cr or more. Curiously, in all cases, the E_{ocp} potential staid in the corrosion domains of Co and Cr (stability of Co^{2+} and Cr^{3+} cations) and not in the corresponding passivation domains

(e.g. CoO/Co $(OH)_2$ or Cr_2O_3/Cr $(OH)_3$). However, by looking again to Figure 2 (right side), one can see that the domain of stability of Cr_2O_3/Cr$(OH)_3$ is very close to the vertical line drawn at pH=2.3 if the corrosion criteria is 1 mol/L of dissolved specie (Cr^{3+}). This is not the case of cobalt the passivation domain of which starts at pH significantly higher (neutral and basic) as this may be seen in Figure 2 (left side). The potential range of proximity between the pH=2.3 vertical line and the chromium passivation domain is [-0.4V; +0.9V] (versus ENH), in which the E_{ocp} of all alloys are included. So, since one can think that initial corrosion may deliver much more Cr^{3+} (and less Co^{2+}) in the vicinity of the working electrode in the case of the three Cr-richest alloys, it appears probable that chromium oxide or hydroxide may precipitate in their case, this promoting the formation of the passivation layer. Since this one is known to be very stable and to remain on surface despite possible decrease in cations later, the Cr-rich alloys can remain passive.

If the passivation layer forms spontaneously over the alloys rich enough in Cr (≥ 20wt.%Cr) it may be induced by severe oxidant attack for the alloys containing Cr is lower quantities. A polarization at rather high potential, artificially applied here with the potentiostat during the first part of the cyclic polarization run, may be achieved with an oxidant strong enough and present a concentration sufficiently high. And after, the formed chromia scale is stable and no depassivation occurs when the applied potential decreases, as demonstrated in the E-decreasing parts of the cyclic polarization curves. Unfortunately, neither the first solution nor the second one, typically of laboratory work, cannot be achieved in mouth without health risk, of course. This is thus compulsory to have at least 20 wt.%Cr in the alloy to be sure to access to the passive state without any special operation.

This threshold chromium content value is may be lower and additional work with alloys containing chromium with contents intermediate between 20 and 15 wt.% (by slices of 2 or 1 wt.%Cr) may lead to answer this question. And In addition, this threshold Cr content can be probably revised downward in case of pH high than the 2.3 considered here. Indeed, by shifting the constant pH vertical line in Figure 3 to the right chromium oxide/hydroxide precipitation (pH = 4 to 5, as some other Fusayama saliva [19,20]) may occur for lower concentrations of Cr^{3+} cations, this authorizing lower Cr content in the alloy. Because of the differential costs between cobalt and chromium (the more expensive of the two), difficulty of melting (Cr is the most refractory out of the two) and the threat of possible precipitation of the brittle Co-Cr sigma phase in some solidification/solid state cooling conditions, less Cr presents some potential advantages. New elements can be also added in small proportions to pre-passive the alloys before chromium oxide/hydroxide precipitation occurs, as the addition of 4wt.%Mo to the 316 austenitic stainless steel does by pre-precipitation of iron molybdate allowing the 316L version to behave as an auto-passive alloy.

Conclusion

Metallic alloys based on unalterable metals such as gold or platinum are used since a long time in dental prostheses. Their undeniable interest was the total absence of corrosion in the buccal milieu, in normal conditions. Since several decades ago one knows that much cheaper alloys may be used instead, but with some requirements for their chemical compositions which must involve metals such as chromium to prevent corrosion. The content in chromium of commercial Ni-based and Co-based Predominantly Base dental alloys varies in a rather broad range, maybe because of the presence of other elements or of not real optimization of the Cr content. Better knowledge of the dependence of the corrosion behavior on the chromium content was the scope of the present study. By discarding the possible influences of other elements, fabrication and use hazards, thanks to a work focused on binary Cobalt-chromium alloys all elaborated and characterized in conditions strictly the same, one succeeded in directly correlating the Cr content and the resulting corrosion behavior, in one of the most representative media for aggressive buccal milieu. It was thus clearly demonstrated that 20wt.%Cr is a minimum chromium content to respect to allow quick and long-lasting passivation of the parts of alloy possibly not covered by the cosmetic part of the prosthese and consequently exposed to the aggressiveness of the buccal milieu. Now long term (several weeks, months…) of free exposures of the passive alloys in acidified Fusayama saliva may be carried out to verify the stability of the chromium oxide/hydroxide scales and the progress of the enrichment of the solution in dissolved species coming from the alloys. To finish one can, say that it can be interesting to reproduce such study for alloys issued from other/new ways of elaborations such as additive manufacturing, laser melting…

References

1. A Prasad (1984) Cobalt-chromium dental alloys. Patent US 4483821.
2. Y S Al Jabbari, T Kotukus, X Barmpagadaki, S Zinelis (2014) Metallurgical and interfacial characterization of PFM Co-Cr dental alloys fabricated via casting, milling or selective laser melting. Dent Mater 30(4): 79-88.
3. MH Reisbick, AA Caputo (1975) Influence of loading rates on mechanical properties of cobalt-chromium alloys. British Densta l Journal 138(8): 295-298.
4. JC Borel, G Cottin, B Coudert, A Dabert, P Herry et al. (1981) Critique of qualification tests for the improvement of the mechanical properties of cobalt-chromium alloys. Me tall Dent (Trav Congr Int) pp. 453-469.
5. S Coletti, J Exbrayat, F Montheillet (1983) Effect of casting method on the fatigue behavior of a cobalt-chromium dental alloy. Materiaux & Techniques 9-10: 219-222.
6. L V J Lassila, P K Vallittu (1998) Effect of water and artificial saliva on the low cycle fatigue resistance of cobalt-chromium dental alloy. The Journal of Prosthetic Dentistry 80(6): 708-713.
7. E Angelini, M Pezzoli, F Rosalbino, F Zucchi (1991) Influence of corrosion on brazed joints strength. Journal of Dentistry 19(1): 56-61.
8. C Laichici, V Tirziu (1968) Structural studies of some cobalt-chromium dental alloys. Stomatologia (Bucur) 15(5): 395-408.

9. D Sun, P Monaghan, WA Brantley, WM Johnston (2002) Potentiodynamic polarization study of the *in vitro* corrosion behavior of 3 high-palladium alloys and a gold-palladium alloy in 5 media. 87(1): 86-93.

10. M F Ayad, S G Vermilyea SF Rosenstiel (2008) Corrosion behavior of as-received and previously cast high noble alloy. J Prosthetics Dent 100(1): 34-40.

11. D Sun, WA Brandtley, GS Frankel, RH Heshmati, WM Johnston (2018) Potentiodynamic polarization study of the corrosion behavior of palladium-silver dental alloys. 119(4): 650-656.

12. F Laurent, B Grosgogeat, L Reclaru, F Dalard, M Lissac (2001) Comparison of corrosion behaviour in presence of oral bacteria. Biomaterials 22(16): 2273-2282.

13. IC Matos, IN Bastos, MG Diniz, MS De Miranda (2015) Corrosion in artificial saliva of a Ni-Cr-based dental alloy joined by TIG welding and conventional brazing. J Prosthetics Dent 114(2): 278-285.

14. C Qian, X Wu, F Zhang, W Yu (2016) Electrochemical impedance investigation of Ni-free Co-Cr-Mo and Co-Cr-Mo-Ni dental casting alloy for partial removable dental prosthesis frameworks The Journal of Prosthetic Dentistry 116: 112-118.

15. L Appelgren, A Dahlen, C Eriksson, N Suksuart, G Dahlen (2014) Dental plaque pH and uratolytic activity in children and adults of a low caries population. Acta Odonatological Scandinavia 72: 194-201.

16. AK Johansson, P Lingstrom, D Birkhed (2007). Effect of soft drinks on proximal plaque pH at normal and low salivary secretion rates. Acta Odontol Scand 65(6): 352-356.

17. International Standard ISO10271:2011(E) (2nd edition: 2011-08-01) Dentistry-Corrosion test methods for metallic materials.

18. (1964) Plenum Press Handbooks of High Temperature Materials. N°1: Materials Index, Plenum Press (New York), USA.

19. HJ Mueller, RW Hirthe (2001) Electrochemical characterization and immersion corrosion of a consolidated silver dental biomaterial. Biomaterials 22(19): 2635-2646.

20. N Schiff, B Grosgogeat, Michele Lissac, Francis Dalard (2004) Influence of fluoridated mouthwashes on corrosion resistance of orthodontics wires. Biomaterials 25(19): 4535-4542.